Journal of the Ceramic Society of Japan 101 [9] 980-984 (1993)

Paper

Structural Characterization and Ion Conductivity of $MCa_2NaNb_4O_{13}$ (M=Rb, Na) with Four Units of Perovskite Layer

Mineo SATO, Yasuhisa KONO and Tetsuro JIN

Department of Material and Chemical Engineering, Faculty of Engineering, Niigata University, 8050, Ikarashi 2-nocho, Niigata-shi 950-21

4層のペロブスカイト骨格をもつ $MCa_2NaNb_4O_{13}$ (M=Rb, Na) の構造解析とイオン伝導性

佐藤峰夫・河野泰久・神 哲郎

新潟大学工学部化学システム工学科，950-21 新潟市五十嵐2の町 8050

[Received April 14, 1993; Accepted June 16, 1993]

Layered perovskite, $RbCa_2NaNb_4O_{13}$, with four units of perovskite layer was synthesized by solid state reaction. A sodium ion-exchanged compound, $NaCa_2NaNb_4O_{13}\cdot 1.7H_2O$, was also synthesized by ion-exchange reaction of a rubidium compound with $NaNO_3$ molten salt. The anhydrous sodium ion-exchanged compound was stable in the temperature range from 350 to 600°C in an ambient atmosphere. The crystal structures of the three materials were determined using the Rietveld method by powder XRD data. The most reliable solutions were obtained for the structural model assuming that the site for a large cation within the perovskite layer, corresponding to the A site for an ideal perovskite, is occupied by the mixed species with the atomic ratio of Ca : Na=2/3 : 1/3. The structures of these compounds are substantially the same as those of $MLaNb_2O_7$ (M=Rb, Na) except for the thickness of the perovskite layer. A fairly high ion conductivity attributed to the interlayer cation was observed at high temperatures for the sodium compound.

Key-words : *Layered perovskite, Ion-exchange reaction, Rietveld analysis*

1. Introduction

Layered oxides derived from the perovskite structure have attracted much attention. A series of such oxides reported by Dion et al.[1] are of the formula $M[A_{n-1}B_nO_{3n+1}]$ of which $KLaNb_2O_7$ [2] and $KCa_2Nb_3O_{10}$ [3] are typical examples for $n=2$ and $n=3$, respectively. The reasons for the interest in these oxides series are that they readily exchange the interlayer alkali ions (Cs, Rb, K) with Na, Li and H. Especially, the corresponding protonated derivatives are interesting because of showing solid Brønsted acidic characters which react with organic bases to form intercalation compounds with large layer expansion.[2),4),5)] Recently, Jacobson et al.[6] have prepared higher member of $M[Ca_2Na_{n-3}Nb_nO_{3n+1}]$ ($n=4$–7) by incorporating additional perovskite layer of NbO_6 octahedra into the parent compound, $MCa_2Nb_3O_{10}$, and have reported the high interlayer reactivity.

In general, many of the compounds exhibiting an ion-exchange reactivity exhibit an ion conductivity as well, such as β-alumina,[7] zeolite[8] and α-zirconium phosphate.[9] In spite of these examples, there has been few investigation on electrical conductive properties for layered perovskite compounds so far, except for our previous studies on $MLaNb_2O_7$ (M=K, Na, H).[10),11)]

In this study we have reported the structural analysis of $MCa_2NaNb_4O_{13}$ (M=Rb, Na) with four units of perovskite layer because the structural refinement of these compounds has not been done, and then have investigated the electrical conductive behavior to know how the ion conductivity depends on the layer thickness.

2. Experimental

$RbCa_2NaNb_4O_{13}$ was prepared by the solid state reaction between $RbCa_2Nb_3O_{10}$ and $NaNbO_3$ powders as reference to the method reported by Jacobson et al.[6] The starting materials for the preparation of $RbCa_2Nb_3O_{10}$ were Rb_2CO_3, CaO and Nb_2O_5. Thoroughly ground mixture of appropriate amounts of Rb_2CO_3, CaO and Nb_2O_5 was pressed into pellets under a pressure of 40 MPa. An excess of 50 mol% of Rb_2CO_3 was added to compensate for the loss due to volatilization of rubidium component. The pellet was placed in an alumina crucible and then heated at 1250°C for 12h in air. After the reaction, the solid product was washed with distilled water to remove an excess of alkaline component and dried in air oven at 100°C. $NaNbO_3$ was prepared by heating the mixture of stoichiometric amounts of Na_2CO_3 and Nb_2O_5 at 1100°C for 3h in air. Finally, using the mixture of equimolar ratio of $RbCa_2Nb_3O_{10}$ and $NaNbO_3$ thus prepared, $RbCa_2NaNb_4O_{13}$ was prepared by heating the mixture at 1200°C for 3h in air.

The ion-exchange reaction to obtain a sodium ion-exchanged compound was done by adding the ground $RbCa_2NaNb_4O_{13}$ powder into a molten salt of $NaNO_3$ at 400°C for 24h. The ion-exchanged product was thoroughly washed with distilled water and then dried at 100°C. The completion of the ion-exchange

reaction was confirmed by X-ray diffraction (XRD) and X-ray fluorescence analyses.

Thermogravimetric analysis (TGA) and differential thermal analysis (DTA) were carried out using a Mac Science thermal analyzer system 001 at a heating rate of $5°C \cdot min^{-1}$ in air.

The powder XRD patterns for the Rietveld analysis were recorded using a Rigaku RAD-rA diffractometer equipped with a high temperature furnace attachment. The Cu Kα radiation used was monochromated by a curved-crystal graphite. The data were collected on thoroughly ground powders by a step-scanning mode in a 2θ range from 3 to 100° with a step width of 0.04° and a step time of 4 s. The powder patterns obtained were analyzed by the Rietveld method, using a RIETAN profile refinement program.[12]

The specimen of $RbCa_2NaNb_4O_{13}$ for the conductivity measurement was a sintered disc prepared by heating a compressed pellet (pressed under 400 MPa) at 1200°C for 3h. The specimen for $NaCa_2NaNb_4O_{13}$ was prepared as follows; the powder of hydrous sodium ion-exchanged compound was first dehydrated by heating at 400°C and then was pelletized by compressing the powder under 400 MPa. The disc thus prepared was of typical dimensions of 10 mm in diameter and about 1.0 mm thick, and two opposite sides of the disc were coated with an evaporated gold film. The conductivity was determined by the complex impedance diagrams obtained by using ac currents in the range from 40 Hz to 100 kHz, using a Hioki 3520 Hi Tester.

3. Results and discussion

3.1 TGA and DTA

Since the sodium ion-exchanged compound has a strong affinity to water molecules, the compound was obtained always as a hydrous form even after drying the ion-exchanged product at 100°C. The parent material of $RbCa_2NaNb_4O_{13}$, however, did not take any hydrous forms even though the compound was washed with distilled water. Fully hydrated sodium ion-exchanged compound is very stable in a wet air. Figure 1 shows the thermal stability of the sodium ion-exchanged compound measured by TGA and DTA. Two endothermic peaks are observed at relatively low temperatures (103°C and 158°C) in the DTA curve. These two peaks correspond to steep weight loss steps in the TGA curve, respectively. The XRD pattern obtained after heating the sample at 300°C shows that diffraction peaks corresponding to the *d*-spacings along the *c*-axis of the crystal shift to the lower side of diffraction angle during exposing it to the ambient atmosphere, e.g., the *d*-spacing for (002) reflection expands from 18.55Å to 20.92Å. This obviously indicates that the water molecules removing in the heating step have a character of water of crystallization. It was found from the weight loss reached finally that the fully hydrated

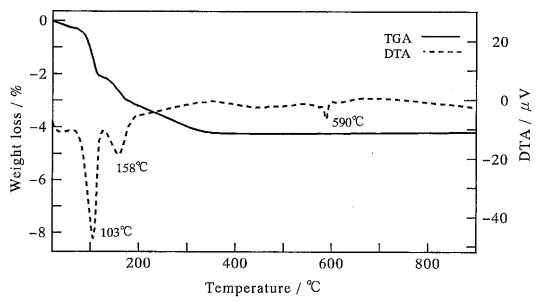

Fig. 1. Thermogravimetric and thermodifferential curves of $NaCa_2NaNb_4O_{13} \cdot 1.7H_2O$.

form has 1.7 water molecules per unit formula, i.e., $NaCa_2NaNb_4O_{13} \cdot 1.7H_2O$. The anhydrous and partially hydrous forms were easily rehydrated in the ambient atmosphere, reforming the fully hydrate. A small endothermic peak is also observed at 590°C. The XRD pattern of the sample heated over this temperature shows the decomposition of the sample.

3.2 Structural analysis

The powder XRD data for the structural refinement were collected at room temperature for $RbCa_2NaNb_4O_{13}$ and fully hydrated $NaCa_2NaNb_4O_{13} \cdot 1.7H_2O$. Since the anhydrate, $NaCa_2NaNb_4O_{13}$, was strong hydroscopic under the ambient atmosphere, the data for this form were collected at room temperature in a high temperature attachment filled with a stream of N_2 gas after the sample was dehydrated by heating at 300°C for 1h. The indexing of the powder pattern obtained was examined with the aid of a computer program CELL.[13] All of the reflections obtained for $RbCa_2NaNb_4O_{13}$ could be assigned as a tetragonal symmetry with the cell parameters approximately equal to $a=3.881$Å and $c=18.906$Å. It was found to be no reflection conditions for this indexing, giving the $P4/***$ type space groups[13] ($P4$, $P\bar{4}$, $P4/m$, $P422$, $P4mm$, $P\bar{4}2m$, $P\bar{4}m2$ and $P4/mmm$). The indexing for $NaCa_2NaNb_4O_{13} \cdot 1.7H_2O$ and $NaCa_2NaNb_4O_{13}$ was also examined. The reflection condition found for both compounds was $h+k+l=2n$ for *hkl* reflections with a tetragonal symmetry, giving the $I***$ type space groups[13] ($I4$, $I4^-$, $I4/m$, $I422$, $I4mm$, $I\bar{4}m2$, $I\bar{4}2m$ and $I4/mmm$). An initial structural model for $RbCa_2NaNb_4O_{13}$ was embodied after some trials on the basis of the assumption that the main perovskite layer constructs perovskite layers with four units analogous to the $CsCa_2Nb_3O_{10}$ which has triple perovskite layers without displacement of each layer. On the other hand, since both sodium ion-exchanged compounds have a body centered Bravais lattice, an initial structural model was constructed by taking into account the displacement of each perovskite layer along the *c*-axis. The Rietveld refinement was done for all space groups given by the CELL results in the first refinement stage. The minimization was done with a modified Marquard algorithm for the refinement. The diffraction

peaks observed at less than $2\theta=10°$ for every compound were eliminated from the calculation because of the large asymmetric effect of peak shape. The early refinement steps for $RbCa_2NaNb_4O_{13}$ showed that the site assignment for sodium and calcium atoms in the perovskite layer, corresponding to the A site for an ideal perovskite, gave the solution with a large negative isotropic thermal parameter for one of the two sites when assuming the individual assignment for these atoms to respective $(0\ 0\ z)$ (Wyckoff notation; $2g$) sites. The most meaningful assignment for these atoms was found when adopting the (Ca, Na) mixed species with the atomic ratio of Ca : Na=2/3 : 1/3. Therefore, this species was also adopted in the refinements for sodium ion-exchanged compounds. In the final refinement stage, positional parameters, isotropic thermal parameters for all atoms and a scale factor were refined. A preferred orientation correction was made because these compounds showed a strong plate-like preferred orientation along with the c-axis due to their layered structure. The most reliable solutions with physically meaningful crystallographic parameters was finally achieved when adopting $P4/mmm$ space group for $RbCa_2NaNb_4O_{13}$ and $I4/mmm$ space group for both sodium ion-exchanged compounds. A typical result of the pattern fitting is shown in **Fig. 2** for $RbCa_2NaNb_4O_{13}$. The crystallographic data and the positional parameters are listed in **Table 1**. The selected interatomic distances and angles are listed in **Tables 2–4**. The R-factors obtained for $RbCa_2NaNb_4O_{13}$ are achieved to reasonably reduced values, while those for both sodium ion-

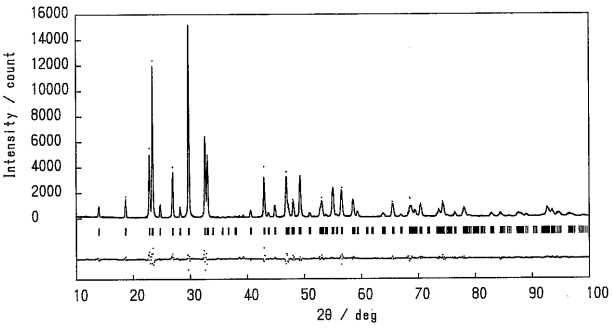

Fig. 2. Powder XRD pattern fitting for $RbCa_2NaNb_4O_{13}$. The calculated and observed patterns are shown on the top solid line and dots. The vertical marks in the middle show positions calculated for Bragg reflections. The trace on the bottom is a plot of the difference between calculated and observed intensities.

Table 1. Positional parameters for $MCa_2NaNb_4O_{13}$ (M=Rb, Na).

Sample	Atom	Site	g	x	y	z	B(A²)
$RbCa_2NaNb_4O_{13}$[1]	Rb	1d	1.0	0.5	0.5	0.5	2.8(4)
P4/mmm	CN(1)[4]	1c	1.0	0.5	0.5	0.0	2.4(8)
a=3.8702(1)Å	CN(2)[4]	2h	1.0	0.5	0.5	0.2229(8)	0.5(4)
c=18.8935(6)Å	Nb(1)	2g	1.0	0.0	0.0	0.1055(3)	0.2(1)
Z=1	Nb(2)	2g	1.0	0.0	0.0	0.3294(3)	0.3(2)
	O(1)	1a	1.0	0.0	0.0	0.0	4(2)
	O(2)	4i	1.0	0.0	0.5	0.103(2)	6(1)
	O(3)	2g	1.0	0.0	0.0	0.203(2)	6(2)
	O(4)	4i	1.0	0.0	0.5	0.307(1)	2.4(9)
	O(5)	2g	1.0	0.0	0.0	0.419(1)	1(1)
$NaCa_2NaNb_4O_{13}\cdot1.7H_2O$[2]	Na	4e	0.5	0.0	0.0	0.275(1)	1(1)
I4/mmm	CN(1)[4]	4e	1.0	0.0	0.0	0.3989(4)	0.2(3)
a=3.8740(1)Å	CN(2)[4]	2b	1.0	0.0	0.0	0.5	0.2(3)
c=41.605(2)Å	Nb(1)	4e	1.0	0.0	0.0	0.0481(2)	0.1(1)
Z=2	Nb(2)	4e	1.0	0.0	0.0	0.1490(1)	0.1(1)
	O(1)	2a	1.0	0.0	0.0	0.0	2.8(5)
	O(2)	8g	1.0	0.0	0.5	0.0471(9)	2.8(5)
	O(3)	4e	1.0	0.0	0.0	0.089(1)	2.8(5)
	O(4)	8g	1.0	0.0	0.5	0.1384(8)	2.8(5)
	O(5)	4e	1.0	0.0	0.0	0.191(1)	2.8(5)
	Ow	8g	0.425	0.0	0.5	0.272(1)	1(2)
$NaCa_2NaNb_4O_{13}$[3]	Na	4d	0.5	0.0	0.5	0.25	4(2)
I4/mmm	CN(1)[4]	4e	1.0	0.0	0.0	0.3857(7)	1.6(7)
a=3.8716(2)Å	CN(2)[4]	2b	1.0	0.0	0.0	0.5	4(1)
c=36.937(2)Å	Nb(1)	4e	1.0	0.0	0.0	0.0541(3)	1.8(4)
Z=2	Nb(2)	4e	1.0	0.0	0.0	0.1680(2)	1.0(3)
	O(1)	2a	1.0	0.0	0.0	0.0	5(4)
	O(2)	8g	1.0	0.0	0.5	0.056(2)	14(3)
	O(3)	4e	1.0	0.0	0.0	0.104(1)	1(1)
	O(4)	8g	1.0	0.0	0.5	0.1568(9)	1(1)
	O(5)	4e	1.0	0.0	0.0	0.218(1)	5(2)

1) R_{wp}=12.42%, R_B=9.02%, R_I=3.42%, R_F=2.35%.
2) R_{wp}=15.61%, R_B=11.59%, R_I=6.06%, R_F=3.11%.
3) R_{wp}=16.69%, R_B=12.98%, R_I=4.31%, R_F=2.78%.
4) The site for (Ca,Na) species with the atomic ratio of Ca:Na=2/3:1/3.

Table 2. Atomic distances and angles for $RbCa_2NaNb_4O_{13}$.

Distance (Å)		Angle (°)	
Rb – O(5)	3.12(1)x4	O(2) – Nb(1) – O(3)	91(1)x4
CN(1) – O(1)	2.736(1)x4	O(2) – Nb(2) – O(2)[i]	89.9(2)x4
CN(1)[1] – O(2)	2.75(2)x8	O(1) – O(2) – O(3)	89.4(8)x4
CN(2)[1] – O(2)	2.96(2)x4	O(4) – Nb(2) – O(5)	102.0(6)x4
CN(2)[1] – O(3)	2.762(8)x4	O(4) – Nb(2) – O(4)[i]	87.5(2)x4
CN(2)[1] – O(4)	2.51(1)x4	O(3) – O(4) – O(5)	93.1(7)x4
Nb(1) – O(1)	1.994(6)	O(2) – O(3) – O(4)	89.7(6)x4
Nb(1) – O(2)	1.935(1)x4		
Nb(1) – O(3)	1.84(5)		
Nb(2) – O(3)	2.38(5)		
Nb(2) – O(4)	1.978(5)x4		
Nb(2) – O(5)	1.70(3)		
O(1) – O(2)	2.75(2)x8		
O(2) – O(2)[i]	2.736(1)x4		
O(3) – O(2)	2.69(3)x4	Symmetry code:	
O(3) – O(4)	2.76(4)x4	none x, y, z	
O(4) – O(4)[i]	2.736(1)x4	i) y, –x, z	
O(5) – O(4)	2.86(2)x4		

1) The site for (Ca,Na) species with the atomic ratio of Ca:Na=2/3:1/3.

Table 3. Atomic distances and angles for $NaCa_2NaNb_4O_{13}\cdot xH_2O$.

Distance (Å)		Angle (°)	
Na – Ow	1.939(4)x2	O(2) – Nb(1) – O(3)	91(1)x4
Na – Ow[i]	2.78(7)x2	O(2) – Nb(2) – O(2)[ii]	89.9(1)x4
Na – O(5)[i]	3.06(4)x4	O(1) – O(2) – O(3)	87.3(9)x4
Na – O(5)	3.46(8)x4	O(4) – Nb(2) – O(5)	102.8(9)x4
CN(1)[1] – O(2)	2.96(3)x4	O(4) – Nb(2) – O(4)[ii]	87.1(4)x4
CN(1)[1] – O(3)	2.78(1)x4	O(3) – O(4) – O(5)	95.6(8)x4
CN(2)[1] – O(4)	2.48(2)x4	O(2) – O(3) – O(4)	88.6(6)x4
CN(2)[1] – O(1)	2.739(1)x4		
CN(2)[1] – O(2)	2.75(2)x8		
Nb(1) – O(1)	2.003(8)		
Nb(1) – O(2)	1.937(1)x4		
Nb(1) – O(3)	1.70(5)		
Nb(2) – O(3)	2.49(6)		
Nb(2) – O(4)	1.987(7)x4		
Nb(2) – O(5)	1.77(5)		
O(1) – O(2)	2.75(2)x8		
O(2) – O(2)[ii]	2.739(1)x4		
O(3) – O(2)	2.60(4)x4	Symmetry code:	
O(3) – O(4)	2.82(4)x4	none x, y, z	
O(4) – O(4)[ii]	2.739(1)x4	i) 1/2–x, 1/2–y, 1/2–z	
O(5) – O(4)	2.94(4)x4	ii) –y, x, z	
O(5) – Ow[i]	2.43(5)		

1) The site for (Ca,Na) species with the atomic ratio of Ca:Na=2/3:1/3.
Symmetry code:

Table 4. Atomic distances and angles for $NaCa_2NaNb_4O_{13}$.

Distance (Å)		Angle (°)	
Na – O(5)	2.26(3)x4	O(2) – Nb(1) – O(3)	878(2)x4
CN(1)[1] – O(2)	2.89(6)x4	O(2) – Nb(2) – O(2)[i]	89.9(1)x4
CN(1)[1] – O(3)	2.759(8)x4	O(1) – O(2) – O(3)	89.8(8)x4
CN(2)[1] – O(4)	2.49(3)x4	O(4) – Nb(2) – O(5)	102(1)x4
CN(2)[1] – O(1)	2.737(1)x4	O(4) – Nb(2) – O(4)[i]	87.4(4)x4
CN(2)[1] – O(2)	2.83(5)x8	O(3) – O(4) – O(5)	94.2(9)x4
Nb(1) – O(1)	1.99(1)	O(2) – O(3) – O(4)	87(1)x4
Nb(1) – O(2)	1.937(2)x4		
Nb(1) – O(3)	1.87(5)		
Nb(2) – O(3)	2.33(5)		
Nb(2) – O(4)	1.979(7)x4		
Nb(2) – O(5)	1.84(5)		
O(1) – O(2)	2.83(5)x8		
O(2) – O(2)[i]	2.737(1)x4		
O(3) – O(2)	2.64(4)x4	Symmetry code:	
O(3) – O(4)	2.72(4)x4	none x, y, z	
O(4) – O(4)[i]	2.737(1) x4	i) –y, x, z	
O(5) – O(4)	2.97(4)x4		

1) The site for (Ca,Na) species with the atomic ratio of Ca:Na=2/3:1/3.

exchanged compounds are fairly large. This is probably due to their relatively poorer crystallinity brought about as a result of the ion-exchange reaction with molten salt.

3.3 Description of structures

The crystal structures of the three compounds refined are shown in **Fig. 3**. All of the structures can be described as layered structure with four units of perovskite, interleaved by alkaline ions. The coordination around rubidium atom is eight-fold coordinated by the oxygen atoms belonging to the perovskite layer. The coordination around sodium atom in the anhydrous sodium compound is an almost perfect regular tetrahedron with 50% site occupancy. These structural features of the above two compounds are substantially the same as those of $MLaNb_2O_7$ (M=Rb, Na),[11),14)] except for the difference in the thickness of the perovskite layer. The situation of the hydrous sodium compound is somewhat complicated. When taking into account only the oxygen atoms forming the perovskite lattice, the coordination around sodium atom is a tetragonal prismatic coordination. The water molecules are statistically distributed in the site forming a square-planar coordination around sodium atom with 50% occupancy. It is difficult to distinguish the accurate positions of sodium atom from those of oxygen atom belonging to a water molecule in the interlayer, owing to the fact that these elements have a smaller contribution to the structure factors obtained by XRD because of their small and almost the same atomic scattering factors. Therefore, it is evident that the structural model proposed here is considered to be substantially correct, but that the accuracy of the atomic positions especially for the atoms located in the interlayer may be still uncertain.

The stacking manner of the layers along the *c*-axis is different between rubidium compounds and sodium compounds; the adjacent perovskite layers are stacked each other without displacement for $RbCa_2NaNb_4O_{13}$ but with displacement by translating by 1/2 along the diagonal direction of the two *a*-axes for both sodium compounds, probably due to the ionic size of the cation located in the interlayer. **Figure 4** shows the environment of niobium atoms in $RbCa_2NaNb_4O_{13}$. There are two types of niobium sites which are crystallographically independent. The NbO_6 octahedra located inside of the perovskite layer are close to an ideal octahedron, while those located outside of the layer are fairly distorted. The Nb–O bonds in the latter octahedra are classified into three types, i.e., a very shortened bond (1.710Å) toward the interlayer space, four normal bonds (1.978Å) linked within the layer and a long bond (2.390Å) toward inside of the layer. These bond characters are more or less seen in the octahedra inside of the layer but its distortion is remarkably depressed. The distortion of the NbO_6 octahedra in the perovskite layer is a quite common feature observed in layered perovskites which exhibit ion-exchange property.[15),16)] The occurrence of the very shortened Nb–O bond can give less charge density to the interlayer space, giving a less interaction between the alkali ion and the perovskite lattice responsible to ion-exchange reaction. The situation in sodium ion-exchanged compounds is something interesting. A large distortion in NbO_6 octahedra is observed for not only the octahedra located inside but also the octahedra located outside in the hydrate (Table 3),

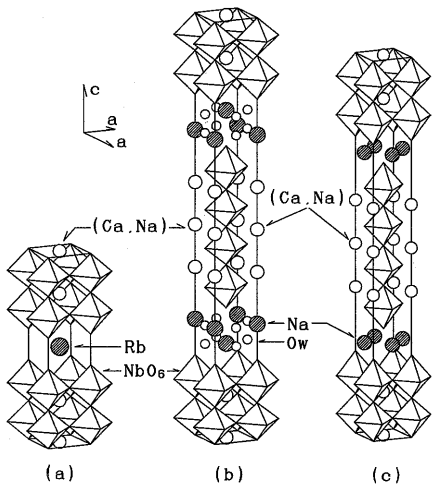

Fig. 3. Crystal structures of (a) $RbCa_2NaNb_4O_{13}$, (b) $NaCa_2NaNb_4O_{13}\cdot 1.7H_2O$, and (c) $NaCa_2NaNb_4O_{13}$.

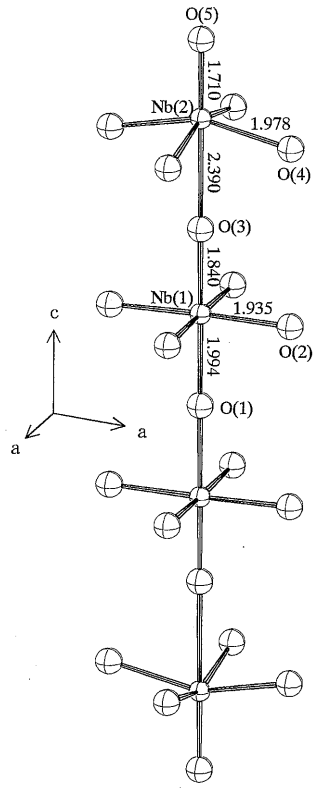

Fig. 4. Environment around niobium atoms in the perovskite layer of $RbCa_2NaNb_4O_{13}$.

while the distortion is fairly relaxed for both octahedra in the anhydrate (Table 4). The origin of the large distortion observed in the hydrate may be due to the existence of the inserted water molecules which may have an interaction with the oxygen atoms of the perovskite lattice by forming some kinds of hydrogen bonds, but the details is unknown at present.

3.4 Conductivity

In the previous study[10] for the analogous layered perovskite, $MLaNb_2O_7$ (M=K, Na, H), it has been known that the proton conduction due to the water molecules adsorbed on the sample occurs at room temperature under a wet atmosphere. In order to pay attention to the ionic conduction attributed to the interlayer ions, the sample was heated once at 400℃ for 30 min before conductivity measurement. The conductivity at room temperature was very low for rubidium and sodium compounds, beyond the range of our measuring apparatus. At elevated temperatures, a large polarization was observed when applying a direct current, implying that an ionic conduction is predominant at high temperatures although the measurement of the ion transport number was not done in this study. **Figure 5** shows the temperature dependence of the conductivity obtained from the Cole–Cole plot analysis for both compounds, together with that for $NaLaNb_2O_7$ as a reference. It is interesting that the conductivity of $NaCa_2NaNb_4O_{13}$ is much higher than that of $RbCa_2NaNb_4O_{13}$, in spite of the compressed sample used for the sodium compound, while a sintered sample was used for $RbCa_2NaNb_4O_{13}$. This conductivity behavior for the sodium compound is considered to come from the fact of not only its small ionic radius but also the 50% site occupancy of sodium site in this crystal. Owing to its layered crystal structure, the ionic motion would be restricted within the interlayer plane where the bottle neck for the ion conduction may be on the edge of NaO_4 tetrahedra. In addition, one can also note that the magnitude of the conductivity and the activation energy observed for $NaCa_2NaNb_4O_{13}$ are quite similar to those observed for $NaLaNb_2O_7$, respectively, even though there is a serious difference in the thickness of the perovskite layer between the two compounds. Such behavior may be comparative with the results of the previous study[6] on the intercalation reactivity of $HCa_2Na_{n-3}Nb_nO_{3n+1}$ ($3 \leqq n \leqq 7$), where a clear correlation between the reactivity and the layer thickness has not been observed. Therefore, it can be concluded that the ion conducting behavior in the layered perovskite compounds is largely independent of the layer thickness but is rather mostly dependent upon the environment around the conductive ions in the interlayer as shown by the structural refinement.

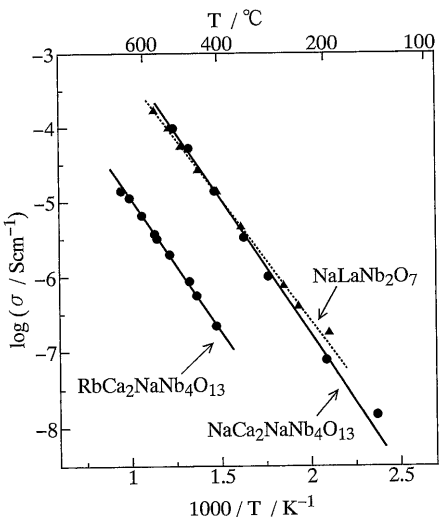

Fig. 5. Temperature dependence of conductivity of $MCa_2NaNb_4O_{13}$ (M=Rb, Na) and $NaLaNb_2O_7$.

Acknowledgements The authors are grateful to Mr. H. Minagawa for his help in data collection of powder XRD measurements and to Dr. Y. Kitayama for her help in DTA and TGA measurements.

References

1) M. Dion, M. Ganne and M. Tournoux, *Mater. Res. Bull.*, **16**, 1429–35 (1981).
2) J. Gopalakrishnan, V. Bhat and B. Raveau, *Mater. Res. Bull.*, **22**, 413–17 (1987).
3) M. Dion, M. Ganne and M. Tournoux, *Rev. Chim. Miner.*, **23**, 61– 69 (1986).
4) A. J. Jacobson, J. T. Lewandowski and J. W. Johnson, *J. Less Common Met.*, **116**, 137–46 (1986).
5) A. J. Jacobson, J. W. Johnson and J. T. Lewandowski, *Mater. Res. Bull.*, **22**, 45–51 (1987).
6) A. J. Jacobson, J. W. Johnson and J. T. Lewandowski, *Inorg. Chem.*, **24**, 3727–29 (1985).
7) G. C. Farrington, B. Dunn and J. O. Thomas, "High Conducting Solid Ionic Conductors, Recent Trends and Applications", Ed. by T. Takahashi, World Scientific, Singapore (1989) pp. 327–65.
8) M. Dekker, T. 'tZand, J. Schram and J. Schoonman, *Solid State Ionics*, **35**, 157–64 (1989).
9) G. Alberti and R. Palombari, *Solid State Ionics*, **35**, 153–56 (1989).
10) M. Sato, T. Jin and K. Uematsu, *J. Solid State Chem.*, **102**, 557–61 (1993).
11) M. Sato, J. Abo, T. Jin and M. Ohta, *J. Alloys Comp.*, **192**, 81–83 (1993).
12) F. Izumi, *Nippon Kesshou Gakkaishi*, **27**, 23–31 (1985).
13) Y. Takaki, T. Taniguchi, H. Yamaguchi and T. Ogura, *J. Ceram. Soc. Jpn. Inter. Ed.*, **95**, 565–71 (1987).
14) M. Sato, J. Abo and T. Jin, *Solid State Ionics*, **57**, 285–93 (1992).
15) M. Dion, M. Ganne, M. Tournoux and J. Ravez, *Rev. Chim. Miner.*, **21**, 92–103 (1984).
16) R. Nedjar, M. M. Borel, A. Leclaire and B. Raveau, *J. Solid State Chem.*, **71**, 182–88 (1987).